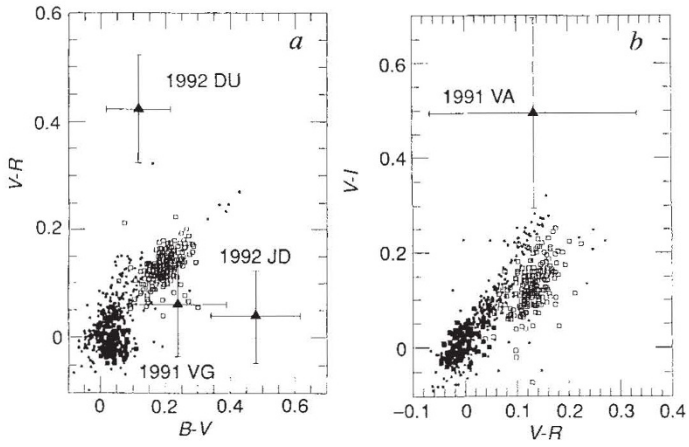

FIG. 3 Magnitude differences through Johnson (B, V) and Cousins (R, I) filters (4,400, 5,500, 6,700 and 8,100 Å, respectively) for small Earth approachers (triangles) and large, main-belt asteroids (solid boxes are spectral type C, open boxes are type S, star-shaped symbols are other types).

of artificial origin because of its extremely Earth-like orbit and unconfirmed evidence for rapid changes in its apparent magnitude, characteristic of artificial satellites[9,10]. Excluding 1991 VG affects none of the above conclusions.

Where does this population of SEAs come from? In ref. 2 it was suggested that they are transported from the main asteroid belt to Earth-approaching orbits by resonant interaction with Jupiter. Owing to their short, collisional lifetimes and enhanced production rate by collisional injection into resonant orbits, an excess would be created with $q \approx 1.0$ AU. It was also suggested that they might be the debris from extinct, short-period comets. However, neither of these explanations accounts for the small eccentricities of the SEAs. New sources may be required, such as lunar ejecta or an undetected population of asteroids at Lagrangian points on the Earth's orbit (analogous to the Trojan groups on Jupiter's orbit).

Further discoveries with the Spacewatch telescope of Earth approachers less than 50 m in diameter are consistent with the distribution of orbits reported here: most have perihelia near 1.0 AU, and many have low eccentricity. As we detect more SEAs with the Spacewatch telescope and observe them photometrically, we will obtain a clearer picture of their orbital distribution and physical properties. This will lead the way to an understanding of their origin. □

Received 19 February; accepted 18 May 1993.

1. Scotti, J. V., Rabinowitz, D. L. & Marsden, B. G. *Nature* **354**, 287–289 (1991).
2. Rabinowitz, D. L. *Astrophys. J.* **407**, 412–427 (1993).
3. Helin, E. F. & Dunbar, R. S. *Vist. Astr.* **33**, 21–37 (1990).
4. Zellner, B., Tholen, D. J. & Tedesco, E. F. *Icarus* **61**, 355–416 (1985).
5. Tedesco, E. F., Gradie, J. G. & Tholen, D. J. *Astr. J.* **87**, 1585–1592 (1982).
6. Landolt, A. U. *Astr. J.* **88**, 439-460 (1983).
7. Landolt, A. U. *Astr. J.* **104**, 340–372 (1992).
8. Keenan, P. C. & McNeil, R. C. *Astrophys. J. Suppl.* **71**, 245–266 (1989).
9. Marsden, B. G. *IAU Circ.* No. 5402 (119).
10. West, R. *ESO Messenger* **66**, 66 (1991).

ACKNOWLEDGEMENTS. We thank D. Sprayberry for observations of 1992 JD, and the National Geographic Society, the Air Force Office of Scientific Research, NASA and the NASA Space Engineering Research Center for support.

One-dimensional reactivity in catalysis studied with the scanning tunnelling microscope

F. M. Leibsle, P. W. Murray, S. M. Francis, G. Thornton* & M. Bowker*

Interdisciplinary Research Centre in Surface Science, University of Liverpool, PO Box 147, Liverpool L69 3BX, UK

THE scanning tunnelling microscope (STM) has yielded great insight into the structure of surfaces and into the dynamics of surface reconstruction and adsorption[1]. We show here that it can also provide direct information about the microscopic mechanisms of catalytic reactions on surfaces. We have studied the oxidation of carbon monoxide on an oxygen-precovered rhodium (110) surface, a process related to the catalytic removal of CO in exhaust gases[2,3]. The STM images show that the reactivity is strongly influenced by the oxygen-induced reconstructions of the surface. The reaction is initiated at high-energy adsorption sites, mainly at steps and domain boundaries of the adsorbed oxygen layer. The CO strips away one-dimensional islands of oxygen atoms on the reconstructed surface, proceeding in the [011] direction. More generally, these results show how the STM can provide insights into the microkinetics of surface reactions.

It is not uncommon for adsorbates to induce movement and reordering of the top layer of metal atoms, and indeed, it generally occurs for oxygen adsorption[1], as this initiates bulk oxidation. A range of other adsorbates also act this way, including C (ref. 4), CO (refs 5, 6) and even hydrogen atoms[7,8]. Gross reconstructions certainly occur when oxygen is adsorbed on Rh(110) as reported earlier[9,10] (see Fig. 1). Our present experiments were done in a commercial ultra-high-vacuum chamber using an Omicron STM, with the rhodium (110) sample being prepared by cycles of argon-ion bombardment and annealing to 650 K. After exposing the sample to 5 langmuirs of oxygen (1 langmuir = 1.32×10^{-6} mbar s) while the sample was maintained at 620 K, a c(2×6) oxygen-induced low-energy electron diffraction pattern could be observed from this surface[9-12]. A scanning tunnelling microscopy image of a typical area of the surface is shown in Fig. 2. Most areas show the c(2×6) oxygen-induced reconstruction, but there are several other types of structure present, including a fairly high density of step edges, terraces, domain boundaries, areas of higher oxygen coverage (c(2×8)), and regions of a (1×2)-type reconstruction.

In Fig. 3, we show more detailed images of these structures. Figure 3 *a* shows an image with both the c(2×6) and c(2×8); these reconstructions[10,12] are modelled by one-dimensional islands of rhodium atoms with adsorbed oxygen atoms interspersed, together with periodic missing rows of Rh atoms in the [011] direction (Fig. 1). Figure 3 *b* is an image of the c(2×8) and (1×2)-type reconstructions. At low oxygen coverages a (2×2) reconstruction is formed and a proposed model involves sub-

FIG. 1 Schematic plans of the proposed Rh structures involved in this work[10,12]. *a*, (1×1) clean Rh(110); *b*, p(2×2) oxygen-induced structure (oxygen atoms are the unfilled circles) showing also the p(1×2) arrangement of surface Rh atoms; *c*, c(2×6); *d*, c(2×8). In all the oxygen-induced structures the top Rh layer has missing rows of Rh atoms in the close-packed direction, compared to the bulk crystal. It is possible that in some structures there is also a zig-zag reconstruction of the Rh atoms with alternate and opposite displacements in the [001] direction. The 3-fold site for oxygen adsorption is indicated by electron energy loss studies [19,20] ▶

*G.T. is also at the Chemistry Department, Manchester University, Manchester M13 9PL, UK. M.B. is also at the Leverhulme Centre for Innovative Catalysis, Department of Chemistry, University of Liverpool, PO Box 147, Liverpool L69 3BX, UK.

© 1993 Nature Publishing Group

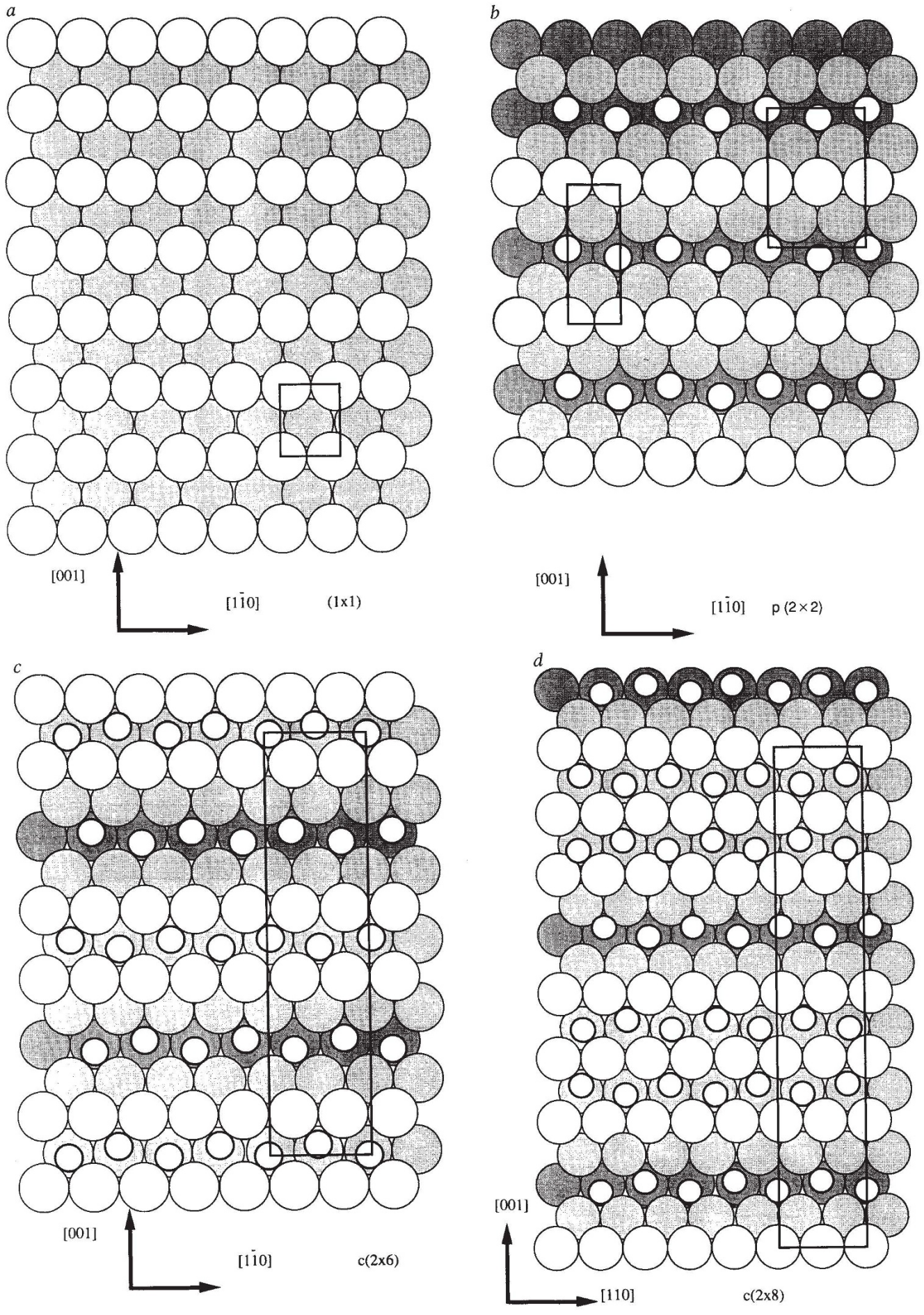

© 1993 Nature Publishing Group

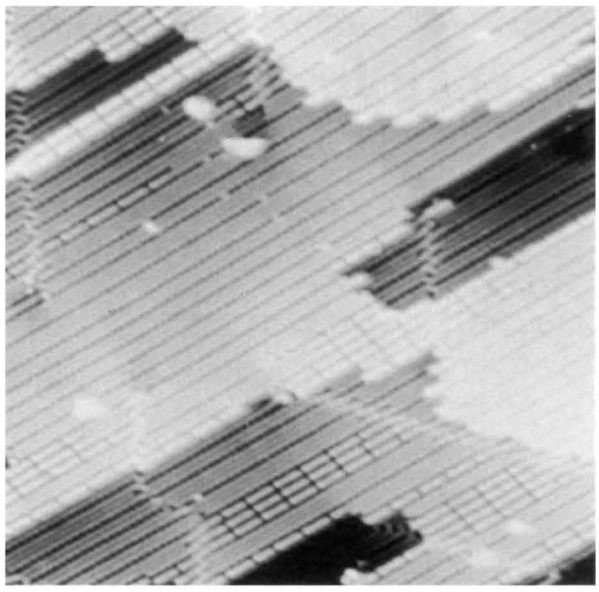

FIG. 2 400 Å × 400 Å scanning tunnelling microscopy image of the oxygen precovered (110) face of rhodium. The oxygen dose used in this experiment mainly produced areas of the c(2×6) reconstruction; also present are areas of the c(2×8) and (1×2) reconstructions. Images were taken with a sample bias of −2.0 V and a tunnelling current of 1 nA. We found that images of the surfaces did not vary significantly with the choice of tunnelling parameters used.

surface oxygen atoms arranged in a (2×2) pattern with top layer rhodium atoms in a (1×2) array[12]. We believe, therefore, that the (1×2) areas that are observed here are actually areas of the (2×2) reconstruction, but that the oxygen atoms are not imaged. At higher oxygen coverages the c(2×6) reconstruction is seen, followed by the c(2×8) and then by the c(2×10)[9,11]. With the oxygen exposure used here, we have converted most of the surface to c(2×6) but there are also areas of higher coverage c(2×8) and lower coverage (1×2). The proportions of the area with the c(2×6), c(2×8) and (1×2) reconstructions are roughly 48%, 35% and 17%, respectively. For many nonlocal probes the presence of multiple reconstructions, step edges and domain boundaries would be a disadvantage, but in scanning tunnelling microscopy, they provide an opportunity for simultaneous experiments on different features.

Carbon monoxide will react catalytically with oxygen on Rh(110), forming carbon dioxide which then desorbs leaving a clean surface[13,14]. Here, we dosed the surface with CO to see how this catalytic reaction proceeded on the different O-induced reconstructions. To do this, we raised the chamber pressure to 1×10^{-8} mbar of CO for ~7 minutes at a sample temperature of 300 K. Figure 4 *a* shows an image of a typical area of the surface after exposure to CO. Bright regions have appeared on the surface. Examination of a higher-resolution image of one of these areas (Fig. 4*b*) shows that the bright regions are bounded by the missing rows and that areas of c(2×6) and c(2×8) coexist around them. This indicates that these lines appear bright not because of a tip effect but because of a real change on the sample. We believe that CO has removed the oxygen within these regions, so they represent either patches of clean surface or of surface with adsorbed CO. These patches are blurred, either because of the delocalized nature of the metal conduction-band electrons or because the CO is vibrating or translating during the time taken to image the surface. Our interpretation is supported by the results of Ertl[15], who showed that the work function of the surface is lower for clean or CO-covered Pt(110) than for the oxygen-covered sample. In this case it would appear that the reaction proceeds linearly in the direction of the missing rows. The longest reacted line measured was 430 Å.

Examination of the width of the reacted region in Fig. 4*b* shows that it is part of a c(2×8) area. Within a fixed area (2×10^6 Å^2) of the sample, we found that the ratio of reacted c(2×6) areas to reacted c(2×8) areas was 1 to 4.3. Weighting the reacted areas with the ratio of percentage areas converted to the two reconstructions, we find that the c(2×8) reconstruction is roughly 6 times more reactive to CO oxidation under the conditions of the experiment. The average lengths of reacted lines were ~91 ± 43 Å and ~89 ± 46 Å for the c(2×6) and c(2×8) respectively. This near-equal average reacted length suggests that once the reaction is initiated, it proceeds with similar velocity along areas of both reconstructions. We saw little evidence for reactions occurring on the (1×2) regions, in agreement with a previous Auger electron spectroscopy study[12].

The data also allow us to infer something about the initiation sites for the reaction. For both the clean and oxygen-reconstructed surfaces, step edges running parallel to the close-packed [011] direction are long and straight, whereas they are ragged in the [001] direction. Of 228 reacted lines examined, all but 37 had a boundary at a [001] step edge or domain wall. This suggests that these features serve as initiation sites for the oxidation process. Furthermore, sequential studies show the reaction front proceeding away from the step edge. It is likely that the steps represent the only free Rh sites available for the adsorption of CO which then enables the reaction to take place.

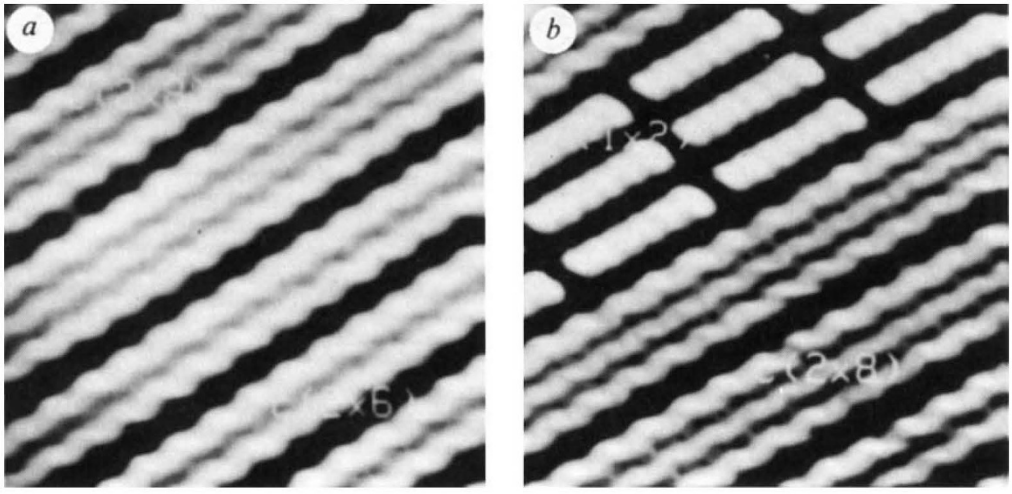

FIG. 3*a*, 60 Å × 60 Å image with the c(2×8) reconstruction present in the upper part of the image and the c(2×6) present in the lower part. *b*, 60 Å × 60 Å image showing both the (1×2) and c(2×8) reconstructions. The segmented nature of the (1×2) reconstruction is not understood.

© 1993 Nature Publishing Group

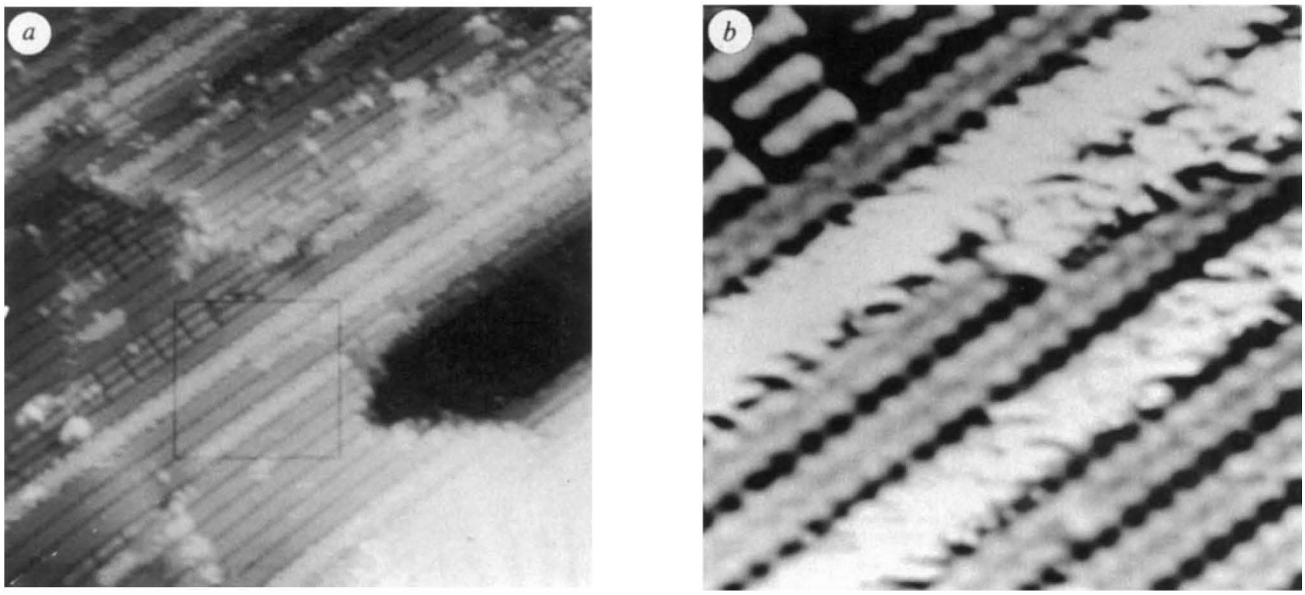

FIG. 4*a*, Typical 400 Å × 400 Å image of an area of the surface following a 5 langmuir exposure to CO. The reaction appears to proceed in a highly directional manner on the surface. Reacted areas appear as bright, blurred lines. *b*, Expanded view of the area contained within the box shown in *a*. This 105 Å × 105 Å image shows reacted c(2×8) and c(2×6) areas coexisting with unreacted c(2×6) and (1×2) areas.

The reason that the step edges at the c(2×8) areas react fastest is probably a lower activation barrier to the O clean-off reaction[13].

That the detailed nature of surface steps can play a critical role in catalytic reactions has been noted previously, for example in the hydrogenolysis of cyclohexane[16]. Although CO oxidation on rhodium seems to be structure-insensitive at low temperatures[17], corresponding to high CO coverage, at the higher temperatures relevant to the situation in car exhausts the surface is dominated by oxygen atoms and the reaction is then sensitive to surface structure[18]. These and other studies have demonstrated the very high mobility of surface metal atoms, as manifested in a wide range of adsorbate-induced reconstructions, and it may be that this kind of diffusion creates the active sites during the catalytic process itself. Our results suggest that such processes should be accessible to direct study with the STM. □

Received 29 January; accepted 6 May 1993.

1. Guntherodt, H.-J. & Weisendanger, R. (eds) *Scanning Tunnelling Microscopy I* (Springer, Berlin 1992).
2. Taylor, K. C. *Catalysis* (eds Anderson J. R. & Boudart, M.) Vol. **5**, 119–170 (1984).
3. Joyner, R. W., Bowker, M. & Truex, T. J. *Chem. Brit.* **28**, 1011 (1992).
4. Onuferko, J. H., Woodruff, D. P. & Holland, B. W. *Surf. Sci.* **87**, 357–374 (1979).
5. Raval, R., Haq, S., Harrison, M., Blyholder, G. & King, D. A., *Chem. Phys. Lett.* **167**, 391–396 (1990).
6. Gaussmann, A. & Kruse, N. *Catal. Lett.* **10**, 305–316 (1991).
7. McIntyre, B. J., Salmeron, M. & Somorjai, G. A. *Catal. Lett.* **14**, 263–269 (1992).
8. King, D. A. & Thomas, G. *Surf. Sci.* **92**, 201–236 (1980).
9. Bowker, M., Guo, Q. & Joyner, R. W. *Surf. Sci.* **253**, 33–43 (1991).
10. Murray, P. W. *et al. Phys. Rev. B*, May 1993 (in the press).
11. Schwartz, E., Lenz, J., Wohlgemuth, H. & Christmann, K. *Vacuum* **41**, 167–175 (1990).
12. Comelli, G. *et al. Surf. Sci.* **260**, 7–13 (1992).
13. Bowker, M., Guo, Q. & Joyner, R. W. *Surf. Sci.* **280**, 50–62 (1993).
14. Bowker, M., Guo, Q., Pudney, P. & Joyner, R. W. in *Studies Surf. Sci. Catal.* **71**, 409–416 (1991).
15. Ertl, G. *Catal. Lett.* **9**, 219–230 (1991).
16. Blakely, D. & Somorjai, G. A. *J. Catal.* **42**, 181 (1976).
17. Oh, S., Fisher, G., Carpenter, J. & Goodman, D. W. *J. Catal.* **100**, 360–376 (1986).
18. Bowker, M., Guo, Q. & Joyner, R. W. *Catal. Lett.* **18**, 119–124 (1993).
19. Cautero, G., Astaldi, C., Rudolf, P., Kiskinova, M. & Rosei, R. *Surf. Sci.* **258**, 44–57 (1991).
20. Comelli, G. *et al. Surf. Sci.* **269/270**, 360–363 (1992).

ACKNOWLEDGEMENTS. This work was supported by the UK SERC and Johnson-Matthey PLC.

Nitrogen transport by vertically migrating diatom mats in the North Pacific Ocean

Tracy A. Villareal*, Mark A. Altabet† & Karen Culver-Rymsza‡

* Environmental Sciences Program, University of Massachusetts, 100 Morrissey Boulevard, Boston, Massachusetts 02125, USA
† Woods Hole Oceanographic Institution, Woods Hole, Massachusetts 02543, USA
‡ Graduate School of Oceanography, University of Rhode Island, Narragansett, Rhode Island 02882, USA

PHYTOPLANKTON production in the surface waters of stratified oceans is fed mainly by nitrogen that has been recycled within the euphotic zone[1]. The nitrogen that is lost from surface waters as organic matter exported to the deep ocean must be balanced by inputs of new nitrogen to the upper ocean[2,3]. Sediment trap studies[2] have shown that the $^{15}N/^{14}N$ ratio ($\delta^{15}N$) of the exported organic matter is higher than that of the suspended particulates, and suggest that the rich nitrate pool below the euphotic zone is the source of 'new' nitrogen for the upper ocean. Yet steep vertical concentration gradients suggest that diffusive upward transport of nitrate is extremely limited, raising the question of how the nitrate reaches the surface waters. Here we present evidence that abundant diatom (*Rhizosolenia*) mats migrate vertically between surface waters and deep nitrate pools in the central North Pacific Ocean. Rising mats contain significantly larger internal nitrate pools than sinking mats. Mat $\delta^{15}N$ is similar to that of the sub-nitricline nitrate, and consistently heavier than that of near-surface particulate organic matter. We conclude that *Rhizosolenia* mats may transport the equivalent of 50% of the new nitrogen requirements into the surface waters of the North Pacific gyre.

Rhizosolenia mats are buoyant, macroscopic (1–30 cm wide) diatom associations of multiple *Rhizosolenia* species occurring over broad expanses of the North Atlantic, North Pacific and Indian oceans[4–6]. Mats are sporadic and occur at 10^{-3} m^{-3} or less

© 1993 Nature Publishing Group